Two-dimensional atomic lithography by submicrometer focusing of atomic beams

Will Williams and M. Saffman

Department of Physics, 1150 University Avenue, University of Wisconsin-Madison, Madison, Wisconsin 53706

Received June 3, 2005; revised January 20, 2006; accepted January 31, 2006; posted February 7, 2006 (Doc. ID 62587)

We analyze a method for serial writing of arbitrary two-dimensional patterns using optical focusing of a collimated atomic beam. A spatial light modulator is used in a side illumination geometry to create a localized optical spot with secondary maxima that are well separated from the central peak. Numerical simulation of a lithography experiment using a magneto-optical trap as a source of cold Cs atoms, collimation and cooling in a magnetic guide, and optical focusing predicts FWHM pixel sizes of 110×110 nm and writing times of $\sim$20 ms/pixel. © 2006 Optical Society of America

OCIS codes: 220.3740, 140.3320.

1. INTRODUCTION

Controlling the motion of neutral atoms using light fields has been an important topic in atomic physics for several decades. Focusing of atoms from a source onto a planar substrate can be used for lithography where the writing is done by an atomic beam instead of a light field. This technique is potentially useful for fabrication of structures with submicrometer resolution. Atomic focusing can be achieved with magnetic or optical fields. In atomic lithography with light fields, an optical profile creates a spatially dependent dipole force that alters the trajectories of neutral atoms. One- and two-dimensional standing-wave light patterns have been used to create periodic atomic patterns.[1–5] Imaging of an atomic beam is also possible using a magnetic lens as was demonstrated by Kaenders *et al.*,[6] and a wide range of atomic guiding and imaging tasks have been demonstrated using magnetic fields.[7]

Although there has been a great deal of work in atomic lithography (recent reviews can be found in Refs. 8–10), only spatially periodic or quasi-periodic[3,11] patterns have been demonstrated. As this limits the range of applications and usefulness of the technique, there is considerable interest in devising approaches that will allow spatially complex structures to be created. One approach to creating nonperiodic patterns is to use a more complex optical field, as in Refs. 12 and 13. An alternative serial writing approach is to focus the atomic beam to a very small spot and then move the spot to draw an arbitrary two-dimensional structure. Spot motion can be achieved either by scanning the spot over a stationary substrate or by moving the substrate. An example of an optically scanned atomic beam focused to a size of $\sim$200 μm can be found in Ref. 14. To obtain higher resolution, tightly focused atomic beams are necessary that can be created by propagation in hollow-core fibers,[15] which have the drawback of low atomic flux, or using Bessel beams.[16–19] A drawback of the Bessel beam approach is the existence of secondary maxima that can lead to atom localization in rings surrounding the central peak.

In this paper we analyze a new approach to focusing an atomic beam to a spot with a characteristic size of $\sim$100 nm. The optical profile used for the atomic focusing is created with a spatial light modulator (SLM) that allows the spot to be scanned with no mechanical motion. By controlling both the phase and the intensity profile of the incident beam, we create an optical funnel that focuses a high percentage of the atomic flux into a single spot. The proposed approach, as shown in Fig. 1, uses a magneto-optical trap (MOT) as a source of cold atoms. A continuous flow of atoms is pushed out of the MOT[9,20,21] and collimated using a magnetic guide followed by an optical focusing region. The magnetic waveguide creates a micrometer-sized atomic beam, with the final focusing down to a full width at half-maximum (FWHM) atomic spot size of $w_{a,\mathrm{FWHM}}=110$ nm provided by a far detuned optical profile. It is then possible to move the optical profile and write a two-dimensional pattern by changing the phases of the laser beams with the SLM. We study the feasibility of this approach using numerical simulations of the atomic trajectories including propagation and cooling in the magnetic guide and the optical profile.

In Section 2 we summarize the main features of optical focusing of atoms and describe the creation of a Bessel profile using side illumination with a SLM. The optical funnel for reduction of atomic trapping in secondary maxima is described in Section 3. The design of a cold atom setup coupled to a magnetic waveguide and then followed by the optical funnel is described in Section 4. Numerical results showing the feasibility of writing a two-dimensional structure are given in Section 5, followed by a discussion of the results obtained and writing speed in Section 6.

2. OPTICAL POTENTIAL

The goal of optically mediated atomic lithography is to control the trajectories of atoms by means of light fields. A collimated atomic beam is passed through a region of spatially varying optical intensity that modifies the atomic trajectories such that a desired atomic pattern is depos-

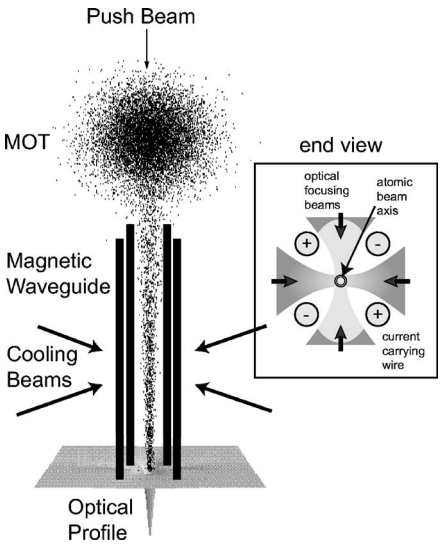

Fig. 1. Proposed method for focusing neutral atoms to a small isolated dot.

ited on a substrate. The conservative optical potential for a two-level atom including the effects of saturation is[22]

$$U = \frac{\hbar\Delta}{2}\ln\left[1 + \frac{I}{I_s}\frac{1}{(1+4\Delta^2/\gamma^2)}\right], \quad (1)$$

where I_s is the saturation intensity, γ is the natural linewidth, $\Delta=\omega-\omega_a$ is the detuning from resonance, ω is the optical frequency, and ω_a is the atomic transition frequency. We write the intensity as $I=I(x,y)g(z)$ where $I(x,y)$ gives the dependence in the x,y plane and $g(z)$ is an envelope function that describes the intensity profile along the z axis, which we will take to be the propagation direction of the atomic beam. Atoms propagating through a region of spatially varying intensity experience a dipole force $\mathbf{F}=-\nabla U$ that alters their trajectories and can be used to focus the atoms into a desired pattern. When $\Delta<0$ (red detuning) we get an attractive potential that concentrates the atoms where the intensity is highest, while for $\Delta>0$ (blue detuning) the potential is repulsive. For potentials of interest we calculate the atomic trajectories numerically using the classical equations of motion for the atomic center of mass. It is also assumed that the atoms do not collide and only interact with the given potential. Therefore, each atom trajectory can be treated individually, and a large number of single atom trajectories resulting from a statistical distribution of initial conditions can be combined to determine an output distribution.

The optical potential can be constructed by combining several laser beams. When only a few beams are used, the potential has a periodic structure, e.g., a one-dimensional standing wave created by two counterpropagating beams, or a checkerboard pattern created by four beams. To focus all of the atoms to a single spot, the periodic structure must be removed. This can be done by adding more laser fields. Consider a two-dimensional field formed using N laser beams all propagating in the same plane and arranged to cross at a common point. The shape of the resulting intensity profile is determined by the angles between the beams as well as the magnitude and phase of the fields. The simplest possibility is to cross the laser beams, which all have equal electric field phases and magnitudes, with equal angular spacing. As the number of beams goes to infinity, the intensity profile tends to $J_0^2(k\sqrt{x^2+y^2})$, the square of the zeroth-order Bessel function that has a ring structure whose scale is dependent only on the wavelength of the light through $k=2\pi/\lambda$. An axicon can be used to create a Bessel beam for this purpose,[18] and it is possible to create higher-order Bessel profiles such as a J_1 profile as proposed by Okamoto *et al.*[19] by altering the phase profile of the beam.

An alternative approach to creating a Bessel beam, as well as more general profiles, is to use a SLM. There has been substantial recent interest in using SLM technology in atom optics[23] as well as an experimental demonstration of manipulation of atoms in microscopic optical traps.[24] Superpositions of Bessel functions may also be useful for addressing individual atoms in optical lattices.[25] Referring to the geometry of Fig. 2, we use linear SLMs, or a single SLM that has been divided into four effective linear segments using mirrors, to create N individually controllable beams that are arranged to cross on

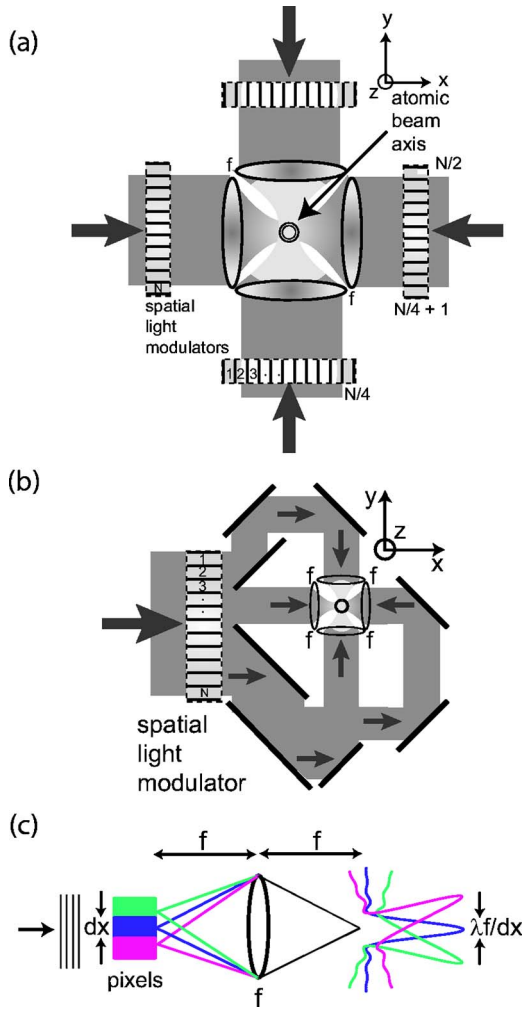

Fig. 2. (Color online) Atomic lithography with four SLMs, each with (a) $N/4$ pixel or (b) a single N pixel modulator. Additional relay lenses needed in (b) are not shown for simplicity. In both cases the SLM pixels are Fourier transformed onto the atomic beam axis as shown in (c).

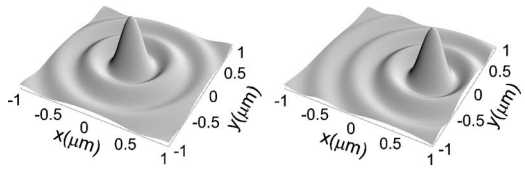

Fig. 3. Example of translating a J_0 Bessel profile composed of 32 laser beams by adding appropriate phase shifts to the interfering plane waves.

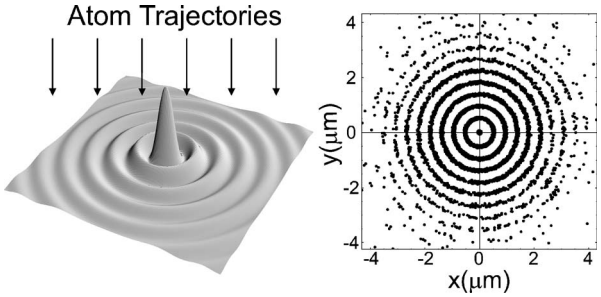

Fig. 4. Atom focusing in two dimensions using a standing wave $I \sim J_0^2(k\sqrt{x^2+y^2})$ light mask. On the right is a numerical example of an atom focusing in the light mask. The atomic beam had an axial velocity of 14 m/s, a transverse distribution with $w_{a,\mathrm{FWHM}} = 1.35\ \mu$m, and a transverse temperature of $T_a = 10\ \mu$K. The peak potential depth is $U/k_B = 21$ mK and the optical mask is created with light of $\lambda = 0.852\ \mu$m.

the atomic beam axis. The beam axis is in a plane that is Fourier conjugate to the SLM as shown in Fig. 2(c). For typical parameters of $\lambda = 1\ \mu$m, $f = 0.1$ m, and $dx = 100\ \mu$m, the sinc function that is the Fourier transform of each pixel has a characteristic width of $\lambda f/dx = 1$ mm. Since this is much larger than the transverse size of the atomic beam (see discussion in Section 4), the atoms are effectively illuminated by N plane waves. Each plane wave has a propagation direction determined by the position of the corresponding pixel and an amplitude and phase that are controlled by the SLM.

When all the pixels are set for the same amplitude and phase, the superposition of beams with uniform angular spacing creates a spot with a Bessel profile as discussed above. When the number of pixels is $N > 32$, the pattern is periodic on scales much longer than the size of the central Bessel peak, so we obtain a well-isolated Bessel profile. After the optical profile is constructed, serial writing of a pattern can be accomplished by translating the central spot where the atoms are focused. The proposed method to accomplish this is to change the phase of each of the individual beams to construct the profile at a new point on the plane. Each beam with index $j = (1, N)$ can be represented as an electric field $E_j = E_0 \exp\{ik[\cos(\theta_j)x + \sin(\theta_j)y] - i\phi_j\}$ where E_0 is the amplitude, k is the wavenumber, ϕ_j is a phase, and θ_j is the angle of the beam propagation direction with respect to the x axis. We assume that all beams are polarized along $\hat{z}$ so we can neglect vectorial effects. To create a Bessel profile centered at $x = y = 0$, we choose all $\phi_j = 0$. To move the profile to be centered at coordinates (x_0, y_0), we put

$$\phi_j = k[\cos(\theta_j)x_0 + \sin(\theta_j)y_0]. \tag{2}$$

This enables translation of the pattern as shown in Fig. 3. Current commercially available SLMs provide 12 bit resolution with as many as several thousand individually adjustable pixels. A SLM can readily be used to create these phase shifts in a side illumination geometry that is compatible with deposition of an atomic beam, as shown in Fig. 2.

The results of a numerical simulation of atom focusing using a J_0^2 Bessel profile can be seen in Fig. 4. Details of the numerical method are given in Section 5. A serious problem with this approach is that the atoms are not focused to a single spot. It is difficult to obtain a large atomic flux in a beam that is narrow enough to prevent focusing into the surrounding ring structure. To correct this, the rings of the Bessel function need to be removed. One possibility is to superimpose a red-detuned J_0 profile with a blue-detuned and repulsive J_1 (or higher-order) profile. The wavelengths and amplitudes of the two Bessel beams can be chosen to suppress the ring structure. While the first ring can be suppressed, higher-order rings are still present and the blue-detuned Bessel profile needs to have a very large detuning. This is because the first maximum of higher-order Bessel profiles is not at the same radius as the first ring of the zeroth-order Bessel. For example, the third-order Bessel has its first maximum at 0.668λ while the first ring of the zeroth-order Bessel is at 0.61λ. Therefore to get the first maximum to line up with the first ring, we must change the wavelength to 776 nm, as compared with the 852 nm used for J_0 focusing with Cs atoms. Since the potential is proportional to $1/\Delta$ for large detuning, the power required to obtain the correct well depth to cancel the first-order ring is extremely large.

3. OPTICAL FUNNEL

In this section we discuss an alternative profile that uses traveling waves to avoid the ring structure that mars the applicability of the Bessel profile. We call this structure an optical funnel. The central spot of the Bessel-squared profile has a FWHM diameter $w_{\mathrm{FWHM}} = 0.359\lambda$. This small width may be relaxed in exchange for a profile that has a less troublesome ring structure. One possible optical profile is the funnel shown in Fig. 5. The funnel is a traveling-wave field that subtends an angular range of π and has amplitudes that decrease linearly on either side of the maximum as compared with the Bessel profile whose beams subtend the full 2π and have equal amplitudes. The radius of the rim of the funnel depends on how many beams are used to create the profile, as shown in Fig. 6. All atoms that enter the profile inside the rim will be funneled toward the point of lowest energy at the cen-

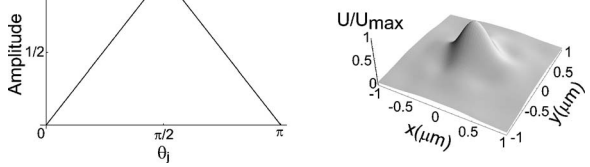

Fig. 5. Optical funnel profile has wave amplitudes that subtend an angular range of π (left), resulting in a localized potential well without secondary rings (right).

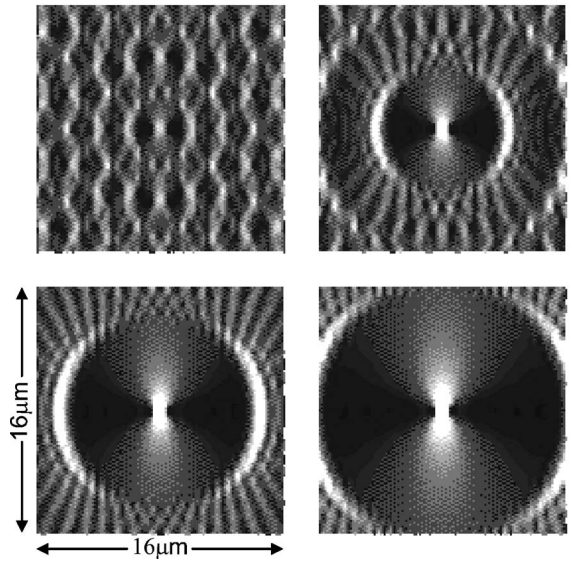

Fig. 6. Optical funnel intensity with lighter regions representing higher intensity. The rim of the funnel has a larger radius as the number of laser beams is increased. The panels show the intensity profile due to 8 beams (top left), 16 beams (top right), 24 beams (bottom left), and 32 beams (bottom right). All panels show a region of $16\times16\ \mu$m.

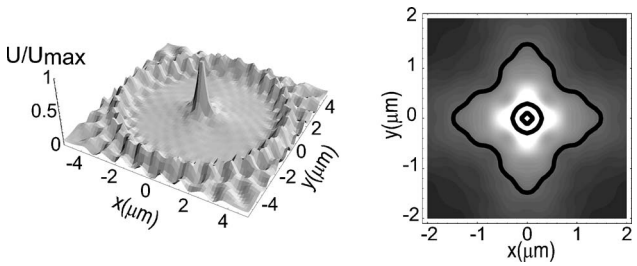

Fig. 7. Symmetrized potential created by the incoherent addition of two funnels (left) and contour plots (right). Contours for 10%, 50%, and 90% of the peak intensity are shown. The optical profile is composed of two noninteracting optical funnels (with different detunings), each composed of 16 laser beams.

ter. The result is a high percentage of the atomic flux being directed into the central spot. The width of the atomic spot that is written then scales as $w_{a,\mathrm{FWHM}}\sim w_{\mathrm{FWHM}}\sqrt{k_BT_a/U_0}$, where U_0 is the maximum well depth of the funnel, and T_a is the temperature of the transverse atomic motion. The FWHM of the funnel intensity profile is 0.48λ in x and 1.38λ in y. We can create an approximately circular potential by combining two noninteracting funnels (they have a relative detuning that is large compared with γ, yet small compared with Δ) to obtain $w_{\mathrm{FWHM}}=0.72\lambda$ in both the x and y directions, as shown in Fig. 7.

Even though the width of the symmetrized funnel profile is approximately twice that of the Bessel profile, this optical potential is preferred since it is possible to focus a large percentage of the atomic flux in a single spot with no rings. Figure 8 shows focusing to a single spot using the same atomic beam parameters as in Fig. 4. For the simulation, two noninteracting funnel profiles are placed on top of each other to create a symmetric potential, as described above. The atomic spot in the funnel has $w_{a,\mathrm{FWHM}}=110$ nm. Note that the ring structure, which is very pronounced when using a Bessel beam, has been essentially eliminated. Both optical profiles have depths of approximately 21 mK. The results of the simulation show that the funnel captures 98% of the atoms into the $2\ \mu$m $\times2\ \mu$m region compared with only 53.6% for the Bessel profile and with only 8.4% captured in the central Bessel spot.

It is interesting to compare the localized potential created with the funnel to simply using tightly focused Gaussian beams propagating in the x–y plane. The use of Gaussian beams would completely eliminate the background ring problem, but comes at the expense of larger spot size. Experiments with a high-numerical-aperture lens system[26] have demonstrated focusing of a single Gaussian beam to a spot diameter of $w_{\mathrm{FWHM}}=0.86\lambda$. At the focus, the confocal parameter of the beam is larger than the transverse waist so we can superpose two incoherent Gaussians, one propagating along $\hat{x}$ and the other propagating along $\hat{y}$, to create a symmetric optical potential. Because there is a large degree of elongation along the propagation axis, even for such a tightly focused Gaussian, the resulting symmetrized intensity profile has $w_{\mathrm{FWHM}}=1.4\lambda$ along $\hat{x}$ and $\hat{y}$, which is almost twice as big as we obtain for the funnel. Comparing Bessel beams, the optical funnel, and Gaussian beams, we see that the funnel combines a relatively small spot size with large radius rings. In Section 5 we demonstrate that two-dimensional structures can be written by translating the funnel profile.

4. ATOMIC SOURCE AND MAGNETIC PRECOLLIMATION

Most experimental demonstrations of atomic lithography have used an oven as a source of thermal atoms. The atomic beam is then collimated using mechanical apertures and/or transverse laser cooling to create a beam suitable for lithography experiments. At least two experiments[27,28] have also used cold or axially cooled atom sources for lithography experiments. A detailed discussion of the relative merits and requirements of different types of atomic sources for lithography experiments can be found in Ref. 9. Generally speaking, oven-based sources provide higher flux and therefore faster writing

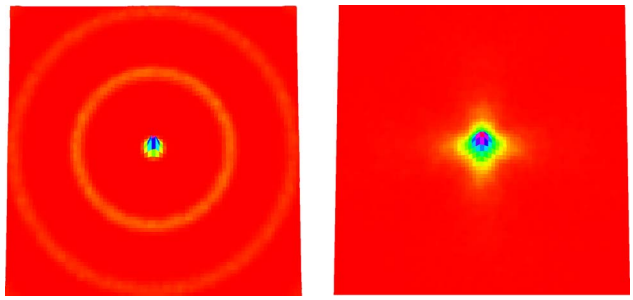

Fig. 8. (Color online) Numerical results for atomic deposition in a Bessel profile (left) and funnel profile (right). Each panel shows a region of $2\ \mu\mathrm{m}\times2\ \mu$m and the optical wavelength is 852 nm. The atomic beam for both figures had a axial velocity of 14 m/s, a transverse distribution with $w_{a,\mathrm{FWHM}}=1.35\ \mu$m, and a transverse temperature of $T_a=10\ \mu$K.

speeds than cold atom sources. One advantage of cold sources is the low longitudinal velocity, which minimizes surface damage and sputtering from atom impact on the deposition substrate. We are interested here in a technique that is suitable for writing feature sizes as small as 100 nm. The requirement for high flux and fast writing over a large area may therefore be less important than minimization of surface effects.

The above considerations motivate us to consider the suitability of a cold atom source using the geometry shown schematically in Fig. 1. To match a MOT source with a transverse size of 0.1–1.0 mm to the micrometer-sized funnel profile so that secondary rings are eliminated, it is necessary to precollimate the atomic beam. We note that this would also be necessary with an oven-based source. We propose to do so using a magnetic guide and transverse laser cooling.

The potential $U(x,y)$ due to a magnetic field $B(x,y)$ in a quadrupole magnetic waveguide is

$$U(x,y) = \mu_B g m B(x,y), \tag{3}$$

$$B(x,y) = b'\sqrt{x^2+y^2}, \tag{4}$$

where $b' = 2\mu_0 J/(\pi a^2)$, m is the magnetic quantum number, g is the Landé factor, μ_B is the Bohr magneton, μ_0 is the magnetic permeability, J is the current, and a is the distance from the center of the guide to each wire. As indicated in Fig. 1, two-dimensional molasses beams are used to cool the atoms in the magnetic guide. The resulting size of the atomic beam after cooling is given by the virial theorem to be

$$<r> = \frac{2k_B T_a}{g m \mu_B b'}. \tag{5}$$

Using numerical values of $J = 500$ A and $a = 4$ mm we get a field gradient of $b' = 25$ T/m, which is approximately eight times larger than what was realized in the experiment of Cren *et al.*[21] With a temperature of $T_a = T_x = T_y = 10$ μK, the estimate found from Eq. (5) for $g = 1/4, m = 4$ agrees extremely well with the numerical data that show the average radial distance of the atoms from the center of the guide to be $<r> = 1.19$ μm.

The magnetic potential is attractive for atoms that are prepared in states with positive m. Since the atoms pass close to the trap axis, we must add a bias field along the longitudinal axis of the guide to minimize Majorana spin flips. The result of this bias field will be a slightly larger atomic beam. The simulations in Section 5 were done with a bias field B_0 to give a total magnetic field $B(x,y) = \sqrt{B_0^2 + b'^2(x^2+y^2)}$. The simulations described in Section 5 show that adding a bias field of $B_0 = 10^{-5}$ T in the axial direction results in a slightly larger average radial distance of 1.26 μm for the above parameters. In the presence of a bias field, the potential is not a homogeneous function of coordinates, so Eq. (5) is not strictly accurate. However, since the bias field is small, the virial prediction is within 5.5% of the numerical result for $T_a = 10$ μK and is an even better approximation for higher temperatures.

5. NUMERICAL RESULTS

Atomic focusing was simulated by numerically calculating the trajectories of individual atoms from the injection into the magnetic waveguide through the optical guide. The atomic parameters were chosen to correspond to the Cs D2 line ($6^2S_{1/2} - 6^2P_{3/2}$) transition with decay rate $\gamma = 2\pi \times 5.22$ MHz. The magnetic waveguide parameters were taken to be $b' = 25$ T/m and $B_0 = 10^{-5}$ T as discussed above. The calculations were performed using a fourth-order Runge–Kutta algorithm.

The atomic beam from the MOT at the entrance to the 35 cm long magnetic guide was taken to be a Gaussian distribution with a $1/e^2$ radius of 100 μm, transverse temperature of 20 μK, and mean longitudinal velocity of 14 m/s. Since compression in the magnetic guide heats the atoms, we added two-dimensional molasses beams to cool the transverse motion. The intensity of the cooling beams was set to 1.09 W/m^2, or $I/Is = 0.1$, and $\Delta_m = -\gamma/2$. The cooling was simulated by randomly changing the velocity of each atom by either $2\hbar k_m/m_a$, $-2\hbar k_m/m_a$, or 0 once per scattering time with probabilities of 25%, 25%, and 50%, respectively, while constantly damping the atoms with a force[29] $-\beta$v. Here k_m is the wavenumber of the molasses beams, m_a is the mass of a Cs atom, and β is the damping coefficient.The velocity kick was added in both transverse directions to independently cool along each axis. Since the axial velocity is relatively high, we neglected the longitudinal heating of the beam, which is estimated to give a spread in the axial velocity of ~ 1.2 m/s.

As a rough approximation for sub-Doppler cooling, the linewidth γ was decreased to artificially decrease the Doppler temperature ($T_D \sim \gamma$). Decreasing γ by a factor of 15 results in a temperature of approximately 10 μK in the transverse plane ($m_a <v_x^2> = m_a <v_y^2> = k_B \times 10$ μK). The resulting FWHM of the atomic beam at the end of the magnetic waveguide is $w_{a,\mathrm{FWHM}} \simeq 1.35$ μm.

Our assumption of the possibility of deep sub-Doppler cooling combined with tight transverse compression in a magnetic waveguide is important for the performance of this approach to atomic lithography. Transverse temperatures as low as 10 μK have been achieved in an experiment with a Cs atomic beam subjected to optical molasses,[30] although this was not done in the presence of a magnetic waveguide. The experiment of Schiffer *et al.* described in Ref. 31 demonstrated cooling of neon atoms to 11 μK together with a root-mean-square beam radius of 42 μm using a field gradient of 3.5 T/m. That work demonstrated that a strong magnetic field gradient did not degrade the performance of sub-Doppler polarization gradient cooling, although the parameter values for which optimum cooling was obtained in the magnetic waveguide were substantially different from those predicted by standard theory.

A theoretical analysis of sub-Doppler cooling in a quadrupole waveguide was given in Ref. 32. Those authors found temperatures of $T_a < 5$ μK and a transverse beam size of 18 μm using a field gradient of $b' = 1$ T/m. The analysis indicates that sub-Doppler cooling should be effective even in the presence of large magnetic field gradients as was observed in Ref. 31. We are assuming a considerably larger gradient of $b' = 25$ T/m to obtain beam widths under 2 μm. Although the previous experimental

and theoretical work supports the possibility of achieving very tight confinement in a steep magnetic guide, it has not yet been demonstrated experimentally. To understand how the lithographic process will be effected by the waveguide performance, we have numerically simulated atom deposition for guide temperatures ranging from 10 to 150 μK, which is greater than the Doppler cooling limit of $T_D=125$ μK for Cs. The corresponding sizes of the beam at the guide exit can be estimated using Eq. (5) to range from ~1.3 to 19 μm.

At the end of the magnetic waveguide we feed the atoms into the optical funnel. The funnel was symmetrized using two noninteracting funnel profiles, each consisting of 32 laser beams. The two funnels are overlapped to form a symmetric potential, as in Fig. 7. The axial profile of the beams was $g(z)=\exp(-2z^2/w_z^2)$, with $w_z=0.6$ mm and their cross section was assumed to be circular in the focusing region. A peak intensity of 7×10^6 W/m^2 and $\Delta/2\pi=-10$ GHz was chosen for one funnel and 6.3×10^6 W/m^2 and $\Delta/2\pi=-9$ GHz for the other. This choice of parameters gives the same well depth for both funnels, but detuned such that they do not interact. This results in a total well depth of $U_0/K_B=21$ mK with a laser power requirement of approximately 124 and 111 mW, respectively. With such a deep well the atomic beam focuses within the optical field as opposed to a thin-lens case, as can be seen in Fig. 9. The temperature of the atoms also increases dramatically inside the funnel. To optimize the atom deposition, the substrate is located within the axial funnel profile where there is nonzero optical intensity. This raises concerns about diffraction from the substrate, but these effects can be minimized by careful attention to experimental parameters (e.g., by using a substrate that is locally raised in an area surrounding the deposition region). All the simulations that follow were obtained with the substrate placed at the center of the Gaussian profile as has been done in some experiments.[33]

When the temperature at the exit of the magnetic guide is $T_a=10$ μK, the lowest temperature considered in the simulations, the resulting number density in the focused spot has $w_{a,\mathrm{FWHM}}=110$ nm as shown in Fig. 10(a). The atoms are distributed with 85.8% of the atoms falling within a radius of 500 nm and 18% falling within the FWHM of the beam. The trajectories of 100 atoms are shown in the inset of Fig. 10(a).

We note that, because of the large intensity of the funnel beams, additional heating due to photon scattering may also be of concern. The peak scattering rate at the center of the many-beam optical funnel is[29]

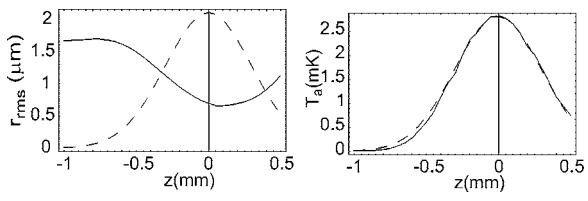

Fig. 9. Root-mean-square width of the atomic beam (left) and transverse temperature (right) of the atoms as they travel through the optical funnel. The initial temperature before entering the funnel is $T_x=T_y=10$ μK. The dashed curves show the axial profile of the funnel potential.

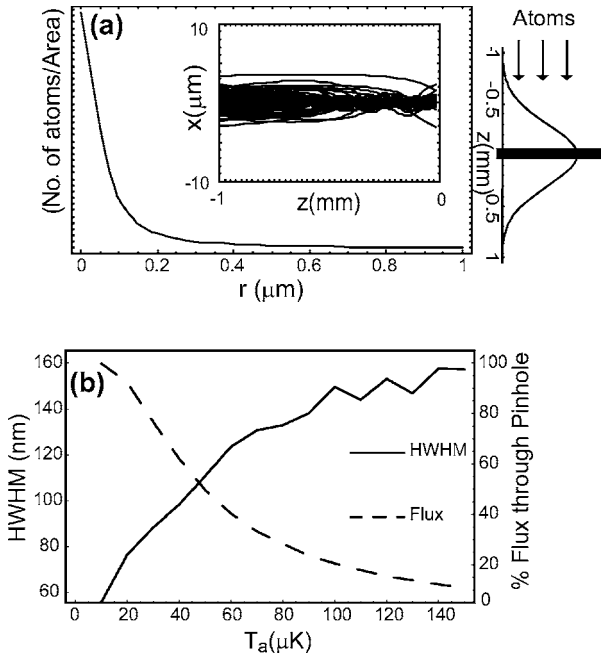

Fig. 10. (a) Number density of the optically focused atomic beam with $w_{a,\mathrm{FWHM}}=110$ nm and $T_a=10$ μK. The insert shows the trajectories of 100 randomly chosen atoms as they travel through the optical profile. The substrate, shown on the right, is in the center of the Gaussian profile. (b) The HWHM of the spot and flux through a 10 μm diameter pinhole are shown as a function of temperature coming out of the magnetic guide.

$$r\sim\frac{\gamma}{2}\frac{\frac{I_0}{I_s}}{1+\frac{4\Delta^2}{\gamma^2}+\frac{I_0}{I_s}}. \tag{6}$$

For the funnel parameters given above, this results in a maximum scattering rate of $r=1.45\times10^6$ s^{-1}. The atom–light interaction time is approximately 0.1 ms and results in scattering of ~150 photons. The scattering of these photons adds $(m_a/k_B)[(\sqrt{150}\hbar k/m_a)]^2=30$ μK to the atomic temperature, which can be neglected since the temperature of the atoms at the center of the profile is approximately 2.5 mK.

Numerical simulations of the atom propagation through the guide show that, as the temperature is allowed to increase, the atoms are also less tightly confined near the axis. This results in an increase of the focused spot size with temperature as shown in Fig. 10(b). When the spread in transverse position at the exit of the magnetic guide becomes comparable to the size of the outer ring of the optical funnel (see Fig. 7), some of the atoms are focused far from the desired location. To prevent this from occurring we have included a mechanical pinhole of diameter 10 μm at the exit of the magnetic guide to block the atoms that are too far from the axis to be focused by the funnel. The resulting loss in flux is shown by the dashed curve in Fig. 10(b). At the low temperatures considered, all atoms pass through the pinhole, which has no effect on the results. At high temperatures the pinhole improves the resolution obtained at the expense of a reduction in flux. We emphasize that the pinhole is assumed spatially fixed and aligned with the magnetic guide, and is not scanned to write the pattern shown below.

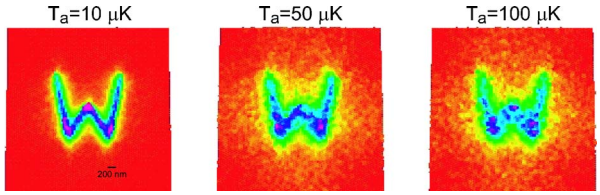

Fig. 11. (Color online) Simulated distribution of atoms deposited to write the letter W written by changing the phases of the beams creating the optical profile. The magnetic guide is stationary and aligned with the center of the picture that shows a region of size 4 μm$\times$4 μm. The indicated temperature is at the exit of the magnetic waveguide.

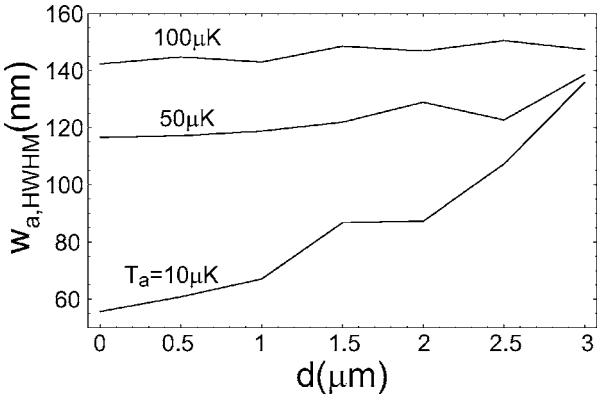

Fig. 12. HWHM of the atomic beam at the substrate as a function of the transverse distance d between the axes of the magnetic waveguide and the funnel.

To simulate writing of a two-dimensional pattern, the optical funnel is reconstructed at varying distances from the atomic beam axis using the phases given by Eq. (2). A simulation of the letter W for several transverse temperatures is shown in Fig. 11. The W is made by positioning the funnel at 101 different spots and depositing a total of 50,500 atoms. We see that the quality of the pattern degrades with increasing temperature, but there is still a clearly resolved shape at temperatures as high as 100 μK.

The FWHM of the atomic beam at the substrate increases the further the optical funnel is from the center of the magnetic guide. Figure 12 shows that, when the beam temperature is 10 μK, the FWHM of the atomic beam on the substrate increases by approximately a factor of 2 when the funnel is moved by a distance of 3 μm. This is because the atoms that enter the potential near the rim obtain a larger radial velocity while traveling to the potential minimum. As a result, the atoms are hotter when they arrive at the substrate and thus have a larger $w_{a,\mathrm{FWHM}}$. This results in a small spreading of the ends of the W, visible for the lowest temperature shown in Fig. 11. For the higher temperatures, motion of the funnel relative to the magnetic guide results only in a small additional increase in the focused spot size.

6. DISCUSSION

We have described an atomic lithography system that uses magnetic and optical fields to focus atoms from a MOT onto a submicrometer spot. Doing so requires combining confining potentials with optical molasses to maintain low atomic temperatures. Using numerical simulations of what we believe to be experimentally feasible parameters, we produce pixels as small as $w_{a,\mathrm{FWHM}}=110$ nm. The position of the pixel can be scanned to write arbitrary planar structures using phase shifts created by a SLM. The optical funnel that produces the final focusing has an acceptance region with a diameter of $\sim$16 μm. However, the funnel cannot be scanned that far since, when the funnel position moves a distance comparable to the width of the beam leaving the magnetic guide, the spot size created by the funnel starts to increase. We can therefore say that for the parameters investigated it appears possible to write no more than several hundred independent pixels with $w_{a,\mathrm{FWHM}}\sim 110$ nm. Alternatively the system could be optimized to write a single small, but stationary spot, and the substrate scanned mechanically. This would in principle allow an arbitrarily large number of pixels to be written. We note that the pixel size predicted here scales with the optical wavelength used for atomic manipulation as well as the kinetic temperature that is attained in the magnetic guide. A number of atomic species are amenable to sub-Doppler cooling techniques. Al and Cr atoms have closed transitions in the ultraviolet, which can be used for optical cooling and guiding. Effective cooling of, e.g., Cr atoms has been obtained that would in principle allow for even smaller pixel sizes than those obtained here for Cs.

For this type of lithography to be practical, the writing speed must not be too slow. Coverage of a surface with one monolayer of Cs corresponds to a surface density of $\sim 4\times 10^{15}$ atoms/cm^2.[33] It has been shown[34] that between three and seven monolayers of Cs are needed to create enough damage for exposure of organic self-assembled monolayer coatings. Given a $T_a=10$ μK spot size of $w_{a,\mathrm{FWHM}}=110$ nm, which defines a pixel with area $\pi(55\ \mathrm{nm})^2=9500\ \mathrm{nm}^2$, the exposure per pixel for one monolayer of Cs is 3.8×10^5 atoms/pixel. Given a flux of 5×10^8 atoms/s and 20% of the atoms falling within an area of diameter $W_{a,\mathrm{FWHM}}$, it will take $\sim$3.8 ms to deposit one monolayer of Cs. The time needed to successfully write three to seven monolayers of Cs to a pixel is then between 11 and 27 ms. The letter W has lengths that total 4.8 μm, which corresponds to at least 4.8 μm/110 nm $\approx$44 spots. Therefore, the writing time for the W would be approximately 1 s. As the temperature increases, so will the writing time due to the loss of flux at the pinhole. For $T_a=100$ μK the flux through the pinhole is reduced by approximately a factor of 5, and the spot area is increased by approximately a factor of 4, which implies an estimated writing time of $\sim$20 s for the W.

A long-term goal of atomic lithography is to produce a large-scale lithographic process. To do so a number of challenges will have to be overcome. The optical funnel will only capture atoms into a small spot if they enter the funnel close enough to the center. Theoretically, we could increase the axial thickness of the funnel or increase the laser intensity to increase the range at which the funnel will capture atoms. Experimentally, this is limited by available laser power. Another experimental challenge will be the sub-Doppler cooling that is required in the magnetic waveguide. Although it has been shown experimentally[31] and theoretically[32] that sub-Doppler

cooling is possible with small spot sizes, experiments have not yet demonstrated deep sub-Doppler cooling together with transverse confinement at the level of $1-2\,\mu$m, which is optimum for feeding into the funnel. Requirements on cooling efficiency could be traded off against stronger compression due to larger magnetic fields. This is limited by the ability to run large currents through small wires.

We note that an alternative approach to sub-Doppler cooling in a waveguide may be to alternate the magnetic guide and the cooling beams in time. The sub-Doppler cooling would then occur without disturbance from the magnetic fields. Provided that the switching frequency is high enough, loss of atoms from the guide will be minimized. Approaches based on lithographically patterned wires[7] that will enable waveguides with smaller dimensions may enable fast switching of the fields as well as tight spatial confinement.

In conclusion, we expect that solutions to these issues, as well as further optimization of performance by refinement of parameter, will be possible. Full evaluation of the suitability of the atom optical approach for writing complex structures described here will ultimately rely on experimental tests.

ACKNOWLEDGMENTS

The authors thank Deniz Yavuz for helpful discussions. This work was supported by National Science Foundation grant PHY-0210357 and an Advanced Opportunity Fellowship from the University of Wisconsin graduate school.

The e-mail address for W. Williams is wdwilliams@wisc.edu.

REFERENCES

1. G. Timp, R. E. Behringer, D. M. Tennant, J. E. Cunningham, M. Prentiss, and K. K. Berggren, "Using light as a lens for submicron, neutral-atom lithography," Phys. Rev. Lett. **69**, 1636–1639 (1992).
2. J. J. McClelland, R. E. Scholten, E. C. Palm, and R. J. Celotta, "Laser-focused atomic deposition," Science **262**, 877–880 (1993).
3. T. Schulze, B. Brezger, R. Mertens, M. Pivk, T. Pfau, and J. Mlynek, "Writing a superlattice with light forces," Appl. Phys. B **70**, 671–674 (2000).
4. C. C. Bradley, W. R. Anderson, J. J. McClelland, and R. J. Celotta, "Nanofabrication via atom optics," Appl. Surf. Sci. **141**, 210–218 (1999).
5. S. J. H. Petra, K. A. H. van Leeuwen, L. Feenstra, W. Hogervorst, and W. Vassen, "Atom lithography with two-dimensional optical masks," Appl. Phys. B **79**, 279–283 (2004).
6. W. G. Kaenders, F. Lison, A. Richter, R. Wynands, and D. Meschede, "Imaging with an atomic beam," Nature **375**, 214–216 (1995).
7. E. A. Hinds and I. G. Hughes, "Magnetic atom optics: mirrors, guides, traps, and chips for atoms," J. Phys. D **32**, R119–R146 (1999).
8. M. K. Oberthaler and T. Pfau, "One-, two- and three-dimensional nanostructures with atom lithography," J. Phys. Condens. Matter **15**, R233–R255 (2003).
9. D. Meschede and H. Metcalf, "Atomic nanofabrication: atomic deposition and lithography by laser and magnetic forces," J. Phys. D **36**, R17–R38 (2003).
10. J. J. McClelland, S. B. Hill, M. Pichler, and R. J. Celotta, "Nanotechnology with atom optics," Sci. Technol. Adv. Mater. **5**, 575–580 (2004).
11. E. Jurdik, G. Myszkiewicz, J. Hohlfeld, A. Tsukamoto, A. J. Toonen, A. F. van Etteger, J. Gerritsen, J. Hermsen, S. Goldbach-Aschemann, W. L. Meerts, H. van Kempen, and T. Rasing, "Quasiperiodic structures via atom-optical nanofabrication," Phys. Rev. B **69**, 201102(R) (2004).
12. M. Mützel, S. Tandler, D. Haubrich, D. Meschede, K. Peithmann, M. Flaspöhler, and K. Buse, "Atom lithography with a holographic light mask," Phys. Rev. Lett. **88**, 083601 (2002).
13. M. Mützel, U. Rasbach, D. Meschede, C. Burstedde, J. Braun, A. Kunoth, K. Peithmann, and K. Buse, "Atomic nanofabrication with complex light fields," Appl. Phys. B **77**, 1–9 (2003).
14. H. Oberst, S. Kasashima, V. I. Balykin, and F. Shimizu, "Atomic-matter-wave scanner," Phys. Rev. A **68**, 013606 (2003).
15. M. J. Renn, D. Montgomery, O. Vdovin, D. Z. Anderson, C. E. Wieman, and E. A. Cornell, "Laser-guided atoms in hollow-core optical fibers," Phys. Rev. Lett. **75**, 3253–3256 (1995).
16. J. E. Bjorkholm, R. R. Freeman, A. Ashkin, and D. B. Pearson, "Observation of focusing of neutral atoms by the dipole forces of resonance-radiation pressure," Phys. Rev. Lett. **41**, 1361–1364 (1978).
17. V. I. Balykin and V. S. Letokhov, "The possibility of deep laser focusing of an atomic-beam into the Å-region," Opt. Commun. **64**, 151–156 (1987).
18. B. Dubetsky and P. R. Herman, "Conical lens for atom focusing," Phys. Rev. A **58**, 2413–2416 (1998).
19. K. Okamoto, Y. Inouye, and S. Kawata, "Use of Bessel J_1 laser beam to focus an atomic beam into a nano-scale dot," Jpn. J. Appl. Phys. Part 1 **40**, 4544–4548 (2001).
20. Z. T. Lu, K. L. Corwin, M. J. Renn, M. H. Anderson, E. A. Cornell, and C. E. Wieman, "Low-velocity intense source of atoms from a magneto-optical trap," Phys. Rev. Lett. **77**, 3331–3334 (1996).
21. P. Cren, C. F. Roos, A. Aclan, J. Dalibard, and D. Guéry-Odelin, "Loading of a cold atomic beam into a magnetic guide," Eur. Phys. J. D **20**, 107–116 (2002).
22. J. J. McClelland, "Atom-optical properties of a standing-wave light field," J. Opt. Soc. Am. B **12**, 1761–1768 (1995).
23. D. McGloin, G. C. Spalding, H. Melville, W. Sibbett, and K. Dholakia, "Applications of spatial light modulators in atom optics," Opt. Express **11**, 158–166 (2003).
24. S. Bergamini, B. Darquié, M. Jones, L. Jacubowiez, A. Browaeys, and P. Grangier, "Holographic generation of microtrap arrays for single atoms by use of a programmable phase modulator," J. Opt. Soc. Am. B **21**, 1889–1894 (2004).
25. M. Saffman, "Addressing atoms in optical lattices with Bessel beams," Opt. Lett. **29**, 1016–1018 (2004).
26. N. Schlosser, G. Reymond, I. Protsenko, and P. Grangier, "Sub-poissonian loading of single atoms in a microscopic dipole trap," Nature **411**, 1024–1027 (2001).
27. J. Fujita, M. Morinaga, T. Kishimoto, M. Yasuda, S. Matsui, and F. Shirnizu, "Manipulation of an atomic beam by a computer-generated hologram," Nature **380**, 691–694 (1996).
28. P. Engels, S. Salewski, H. Levsen, K. Sengstock, and W. Ertmer, "Atom lithography with a cold, metastable neon beam," Appl. Phys. A **69**, 407–412 (1999).
29. H. J. Metcalf and P. van der Straten, *Laser Cooling and Trapping* (Springer-Verlag, 1999).
30. F. Lison, P. Schuh, D. Haubrich, and D. Meschede, "High-brilliance Zeeman-slowed cesium atomic beam," Phys. Rev. A **61**, 013405 (2000).
31. M. Schiffer, M. Christ, G. Wokurka, and W. Ertmer, "Temperatures near the recoil limit in an atomic funnel," Opt. Commun. **134**, 423–430 (1997).

32. V. I. Balykin and V. G. Minogin, "Magnetooptical compression of atomic beams," J. Exp. Theor. Phys. **96**, 8–18 (2003) [Zh. Eksp. Teor. Fiz. **123**, 13–24 (2003)].
33. F. Lison, H.-J. Adams, D. Haubrich, M. Kreis, S. Nowak, and D. Meschede, "Nanoscale atomic lithography with a cesium atomic beam," Appl. Phys. B **65**, 419–421 (1997).
34. K. K. Berggren, R. Younkin, E. Cheung, M. Prentiss, A. J. Black, G. M. Whitesides, D. C. Ralph, C. T. Black, and M. Tinkham, "Demonstration of a nanolithographic technique using a self-assembled monolayer resist for neutral atomic Cesium," Adv. Mater. (Weinheim, Ger.) **9**, 52–55 (1997).